

Numerical study of non-linear twisted blades for tidal turbines improvement

Nu Rhahida Arini¹, Philips Ade Putera Atmojo¹, Deni Saputra¹, Dendy Satrio²

¹Department of Mechanical Engineering and Energy, Politeknik Elektronika Negeri Surabaya, Surabaya, Indonesia

²Department of Ocean Engineering, Faculty of Marine Technology, Institut Teknologi Sepuluh Nopember, Surabaya, Indonesia

Article Info

Article history:

Received Nov 3, 2024

Revised May 14, 2025

Accepted Jun 13, 2025

Keywords:

Computational fluid dynamics

Horizontal-axis tidal turbine

Non-linear twisted foil

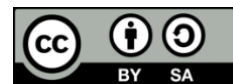
Ocean renewable energy

OpenFOAM

ABSTRACT

Despite the growing demand for renewable energy, the utilization of tidal energy remains underdeveloped due to efficiency limitations in turbine design. Addressing this gap, this study investigates the performance of horizontal-axis tidal turbines (HATT) by comparing two foil designs, National Advisory Committee for Aeronautics (NACA) 2415 and OptA, to optimize energy extraction efficiency. The research employs computational fluid dynamics (CFD) simulations using OpenFOAM to evaluate the effects of foil modifications and non-linear twist distributions on turbine performance across varying tip speed ratios (TSR). The results indicate that the OptA foil significantly improves turbine performance, achieving a 41.4% increase in torque and a 40.2% increase in power coefficient (C_p) at TSR 5, which was identified as the optimal operating condition. The OptA foil enhances velocity distribution, reduces flow separation, and improves vortex behavior, leading to greater efficiency and stability. These findings confirm that foil selection and blade design modifications play a critical role in HATT optimization.

This is an open access article under the [CC BY-SA](#) license.



Corresponding Author:

Nu Rhahida Arini

Department of Mechanical Engineering and Energy, Politeknik Elektronika Negeri Surabaya

St. Raya ITS–PENS Campus, Sukolilo, Surabaya 60111, East Java, Indonesia

Email: arini@pens.ac.id

1. INTRODUCTION

The global energy demand continues to rise, as highlighted by data from the International Energy Agency (IEA). According to the IEA's report, energy consumption per capita increased from 3.2 to 3.4 MWh in 2021, with further growth expected in the coming years [1]. As a developing country, Indonesia is also experiencing notable increases in energy demand. In 2018, per capita electricity consumption stood at 1.06 MWh, rising to 1.09 MWh by 2020 [2]. Currently, conventional steam power plants supply 62% of Indonesia's electricity [3]. However, these plants are set to be phased out by 2060, while the share of renewable energy remains low, accounting for only 13.09% far from the 23% renewable energy target for 2025 [4]. This emphasizes the urgent need to develop renewable energy sources, such as tidal turbines, to meet future energy demands in a sustainable manner.

Tidal energy offers significant potential for harnessing renewable power through horizontal-axis tidal turbines (HATTs), which are generally preferred over vertical axis tidal turbines (VATTs) due to their superior performance. However, the technology remains underdeveloped, and its efficiency still lags behind that of wind energy. Several studies have investigated various methods to enhance HATT performance. According to Myers and Bahaj [5], performance improvements can be broadly categorized into two approaches: control system optimization and fluid dynamics refinement. Control-based enhancements focus on optimizing systems such as yaw control to maximize energy extraction, as demonstrated by Dong *et al.* [6].

On the other hand, fluid dynamics refinement primarily involves modifications to foil design, such as Boudis *et al.* [7] analyzed pressure distribution to improve energy extraction. A key factor influencing turbine efficiency is the foil profile, which directly impacts the lift and drag forces acting on the blades. Goundar and Ahmed [8] emphasized that the lift-to-drag ratio is affected by both the foil shape and the angle of attack, leading to significant variations in turbine performance based on these design parameters.

The selection of an optimal foil is a critical factor in turbine efficiency. Various studies have been conducted to determine the most suitable foil for HATT applications. Tefera *et al.* [9] compared multiple National Advisory Committee for Aeronautics (NACA) foils and concluded that thinner profiles, such as NACA 23012, perform better due to improved pressure distribution. Alipour *et al.* [10] contradicted these findings, demonstrating through computational fluid dynamics (CFD) simulations and experimental validation that NACA 4412 achieves a higher power coefficient (C_p), even approaching the Betz limit. Meanwhile, Gray *et al.* [11] introduced a modified foil, GR4510, which outperformed both NACA 4412 and NACA 2412, reinforcing the hypothesis that pressure distribution along the chord length enhances turbine performance. These studies suggest that thinner foils may improve efficiency, including NACA 2415 for better tidal turbine applications.

The NACA 2415 airfoil, which is widely used in current turbine designs, is a relatively simple, linear foil that provides a balance between lift and drag. However, its performance is limited in terms of maximizing efficiency, particularly under varying flow conditions or when optimized for specific turbine operating points. In contrast, the introduction of non-linear twisted foils represents a significant advancement by offering greater flexibility in blade design. Non-linear twist allows for adjustments in the angle of attack along the length of the blade, optimizing the hydrodynamic performance for different portions of the blade and across different operating conditions. This modification can help reduce flow separation, lessen vorticity in the wake, and enhance the lift-to-drag ratio at varying tip speed ratios (TSRs), leading to improved energy extraction and overall turbine performance. Non-linear twisted foils have the potential to deliver better performance, particularly in complex or turbulent flow conditions, compared to the fixed, linear characteristics of the NACA 2415 airfoil. However, adopting non-linear twists in turbine blade design using NACA 2415 has not been fully understood, especially in the application of HATT. The adoption represents a key area of research and development, bridging the performance gap between existing turbine profiles and next-generation designs optimized for higher efficiency. This study aims to bridge this gap by numerically evaluating and comparing NACA 2415 and its modification using non-linear twists for improving HATT performance.

Recent studies have shown that asymmetric foils can enhance turbine performance, particularly when incorporating blade twisting along the spanwise length [12], [13]. Sun *et al.* [14] demonstrated that a twisted NACA 2415 foil significantly improved efficiency. However, its effectiveness in practical HATT applications has not yet been determined. The fluid behavior around the turbine blades using this profile requires further evaluation to confirm its impact on power output. This research investigates the impact of non-linear twisting on the performance of the HATT blade using the NACA 2415 foil, contributing novel insights into optimizing tidal turbine efficiency.

Conducting physical experiments for tidal energy research is often costly and requires specialized equipment. To overcome this challenge, CFD is widely used to predict turbine performance accurately. Several studies employing CFD for HATT analysis have yielded significant results [15]–[17]. Compared to proprietary software, OpenFOAM provides greater flexibility in customizing solvers for tidal turbine applications, making it a suitable choice for this study [18]. OpenFOAM allows for detailed simulations of real-world environmental conditions, providing valuable insights into turbine behavior before large-scale implementation. Although earlier studies have focused on the influence of airfoil types and linear twist angles, they have not thoroughly explored the hydrodynamic implications of applying non-linear twist along the blade span. The findings from this study aim to enhance the design optimization of tidal turbines, contributing to the progress of renewable energy solutions in Indonesia and supporting broader efforts toward a more sustainable global energy future.

2. DESIGN OF HORIZONTAL-AXIS TIDAL TURBINE BLADE

Designing a HATT blade involves several key factors, including fluid mechanics (aerodynamics and hydrodynamics), material selection, and structural integrity. The design of a HATT blade is aimed at optimizing its efficiency in extracting energy from tidal currents. The blade design must account for the complex flow dynamics of water, similar to the design of wind turbine blades, but with differences in density, flow characteristics, and environmental factors. From a fluid mechanics point of view, the main considerations and the key design objectives include maximizing energy extraction and minimizing drag and flow separation. This will be strongly influenced by blade geometry. Blade geometry plays a significant role in the performance of a tidal turbine. One parameter of blade geometry that is important is the foil profile. The selection of foil is crucial for the lift and drag characteristics thus influence HATT performance.

2.1. Selection of foil profiles for horizontal-axis tidal turbine

The selection of an appropriate foil is critical for enhancing turbine performance. NACA 2415 is chosen for its favorable hydrodynamic characteristics, particularly its superior lift-to-drag ratio, making it well-suited for tidal applications [19]. The NACA 2415 airfoil features a moderate camber and a thin profile, which helps reduce flow separation and improve energy extraction efficiency. Its shape allows for better performance in fluctuating flow conditions commonly found in tidal environments. However, the efficiency of the HATT can be further optimized by modifying the foil profile to better suit specific operational conditions.

Non-linear twist is incorporated into the NACA 2415 airfoil, resulting in the OptA design proposed by Rotor and Hefazi [16]. This modified airfoil aims to minimize cavitation, a critical factor in underwater applications where bubble formation can degrade efficiency and lead to blade erosion. The OptA airfoil features a more complex twist distribution, designed to optimize the angle of attack across the length of the blade. This twist helps maintain optimal hydrodynamic performance, reducing flow separation and increasing lift at different radial sections of the blade, especially under varying tidal current speeds. Additionally, the increased surface roughness of the OptA foil improves boundary layer control, enhancing performance under fluctuating flow conditions by reducing the likelihood of flow detachment and turbulent flow near the surface. In this study, both the NACA 2415 and OptA foils are applied and compared in a HATT. The comparison includes an evaluation of performance under varying TSR and flow conditions. A visual comparison of the foils is presented in Figure 1, illustrating the key differences in profile and design modifications. Figure 1(a) shows the comparison between the NACA 2415 wing profile and the modified wing profile, Figure 1(b) shows the turbine design geometry, and Figure 1(c) shows the distribution of twist angle and chord length of the blade. From Figure 1(a), it can be seen that the OptA airfoil incorporates specific features such as an increased thickness near the root and a tapered design towards the tip, which allows for a better distribution of loads along the blade. These modifications are especially useful for underwater turbines, as they reduce the risk of cavitation while maintaining high C_p s in low-flow conditions.

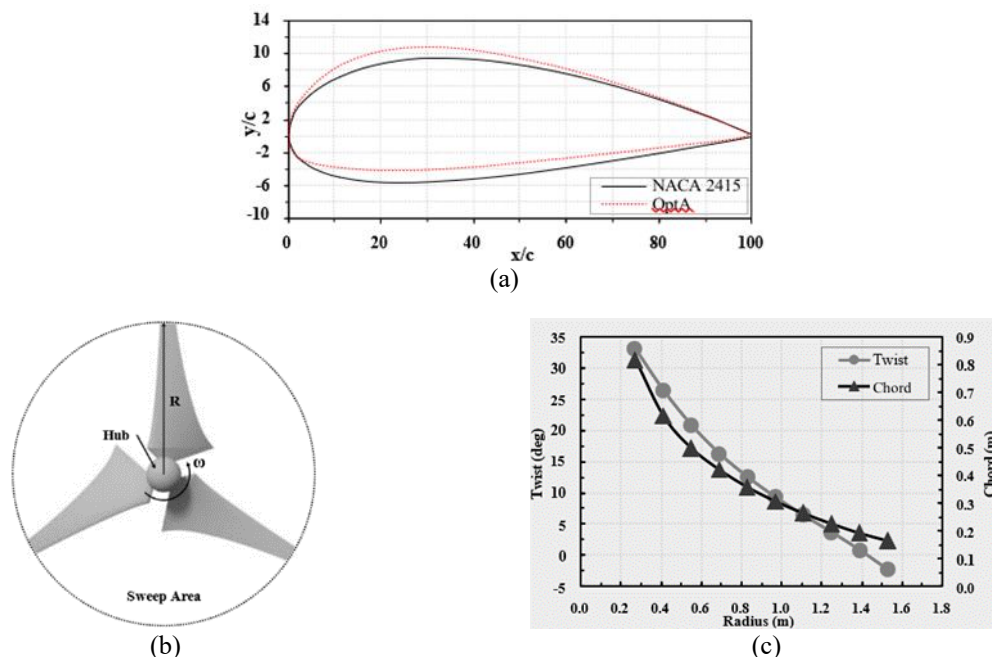


Figure 1. Visual comparison of the foils of (a) comparison between NACA 2415 foil and modified foil [16], (b) turbine design geometry, and (c) distribution of twist angle and chord length of blade [18]

2.2. Blade geometry and twist distribution in horizontal-axis tidal turbine

In the design of a HATT, blade geometry and twist distribution play key roles in determining efficiency and performance. Blade geometry refers to the overall shape and dimensions of the blade, which directly influence its hydrodynamic performance. Key parameters include blade length, chord length, tip and root design, and aspect ratio. Twist distribution, on the other hand, is critical as it affects the angle of attack and hydrodynamic efficiency across the blade span. Proper blade twisting optimizes the angle of attack, reducing flow separation and maximizing energy capture. The twist angle is carefully distributed to maintain

an optimal lift-to-drag ratio along the blade's length, ensuring efficient energy conversion [17]. For HATTs, non-uniform twist is commonly used to adapt the blade's performance to varying radial flow conditions. While some turbine designs use a constant twist, where the angle of attack remains the same along the entire blade, this is less effective for tidal turbines due to variable flow characteristics. In a non-linear twist design, the angle of attack is adjusted along the blade, with a higher angle near the root and a reduced angle at the tip, ensuring optimal hydrodynamic performance across the entire length.

The NACA 2415 airfoil, when applied to HATT blades, must be optimized in terms of both geometry and twist distribution to ensure maximum energy extraction from the tidal flow while maintaining stable operation. The twist distribution on the NACA 2415 is specifically designed to allow the blade to operate efficiently across varying tidal flow conditions. Typically, the twist angle increases toward the root to match the lower water velocities near the hub, while the twist angle decreases toward the tip to reduce the angle of attack and minimize drag at higher velocities, where the water flow is faster. This optimal twist distribution balances lift generation and drag reduction. Excessive twists near the tip can cause high drag, while insufficient twist near the root can lead to flow separation and reduced lift. The twist distribution for NACA 2415 in a HATT design is carefully optimized to account for the varying forces and flow velocities along the blade span. In this study, CFD simulations are used to evaluate different twist profiles and maximize efficiency while minimizing losses. Non-linear twists reduce the likelihood of flow separation at the blade's tip and help maintain a stable lift-to-drag ratio under different operating conditions, ensuring the turbine performs effectively across a range of TSRs.

The fundamental geometric blade profile in this study is derived from the turbine design developed by Sun *et al.* [14], which utilizes the inverse boundary element method (IBEM) theory. Figure 1(b) illustrates the geometric HATT model incorporating the modified NACA 2415 foil, designed using IBEM theory (Figure 1). The turbine rotor consists of three blades, optimized for maximum efficiency, with a spanwise length of 1.55 meters. The specific twist distribution is detailed in Figure 1(c).

2.3. Performance evaluation metrics

Performance evaluation metrics are parameters for assessing the efficiency and effectiveness of HATTs. These metrics help quantify how well the turbine is capturing energy from tidal flows, and they are used to optimize turbine design and operational strategies. Key performance evaluation metrics commonly used for HATTs are TSR, C_P , and torque coefficient (C_T), which are used in this study. TSR, which represents the ratio of the tangential speed of the blade tip to the inlet velocity (U , in meters per second) [20]. The TSR equation is expressed in (1).

$$TSR = \frac{\omega R}{U} \quad (1)$$

$$C_P = \frac{T\omega}{0.5\rho AU^3} \quad (2)$$

$$C_T = \frac{T}{0.5\rho AU^2} \quad (3)$$

Where R and ω denote the turbine radius (in meters) and angular speed (in radians per second), respectively. R remains constant throughout the analysis. Since the inlet velocity is set to 2 m/s, reflecting typical tidal flow conditions found in Indonesian waters, the value of ω will be adjusted for TSR variation accordingly. Two other key performance indicators are the C_P and C_T . The C_T measures the torque generated by the turbine blades relative to the torque that would be produced by an ideal turbine. This metric is useful for understanding the mechanical forces that drive the generator and convert rotational motion into electrical power. Whereas C_P measures how efficiently the turbine converts the kinetic energy of the tidal flow into mechanical power. The C_P is defined as the ratio of the actual power extracted by the turbine to the theoretical maximum power available in the tidal flow. The maximum value of C_P is often referred to as the Betz limit for wind turbines, but for tidal turbines, this value is lower due to the different characteristics of water flow and resistance. A higher C_P indicates better performance and energy extraction efficiency. C_P and C_T are defined as in (2) and (3). Where T is the torque, A is the swept area, and ρ is the density of water, which is 1000 kg/m³.

3. METHOD

The turbine design in this study consists of two distinct configurations: one based on the NACA 2415 foil and the other on a modified NACA 2415 foil with a non-linear twist along the blade (referred to as OptA), as shown in Figure 1(c). The NACA 2415 foil is chosen due to its well-established hydrodynamic characteristics, including a favorable lift-to-drag ratio, while the OptA design incorporates a

non-linear twist to optimize energy extraction by adjusting the angle of attack along the blade span. The generated turbine models, representing both foil configurations, are imported into OpenFOAM, a widely used CFD software, for detailed numerical simulations. These simulations are performed using the pimpleFOAM solver, which is suitable for transient, incompressible flow analysis in turbomachinery applications. A velocity inlet of 2 m/s is applied as the inflow condition to simulate realistic tidal flow velocities in a marine environment. The performance of both turbine designs is systematically evaluated across a range of TSR values, which is crucial for understanding the turbines' operational efficiency under different flow conditions. These simulations provide valuable insights into the effect of airfoil geometry and twist distribution on the turbine's power output, torque, and overall hydrodynamic performance. Additionally, the study aims to assess the influence of varying TSR values on the turbines' ability to extract energy from the tidal flow, ultimately contributing to the optimization of HATTs.

The numerical methodology in this study covers flow equations, turbulence models, meshing strategy, and setting up boundary conditions (BC). Defining these parameters allows the pimpleFOAM solver to accurately model the case in transient and incompressible simulation. Additionally, pimpleFOAM is chosen for its ability to handle unsteady flow conditions, which are typical in tidal turbine applications where the flow velocity can fluctuate with the tidal cycles. The numerical parameters are detailed as follows.

3.1. Flow equations

The dynamic fluid model solves the Navier-Stokes (NS) and the continuity equations. The NS equation, which governs fluid flow within the domain model, is tackled using the finite volume method (FVM) within OpenFOAM solvers. These equations are represented in (4) and (5).

$$\frac{\partial u_i}{\partial x} = 0 \quad (4)$$

$$\frac{\partial(\rho u_i)}{\partial t} + \frac{\partial(\rho u_i u_j)}{\partial x_j} = -\frac{\partial P}{\partial x_i} + \partial(2\mu S_{ij} - \rho u_i u_j) \quad (5)$$

Where u_i represents the mean velocity component, P denotes the mean pressure, μ signifies the kinematic viscosity, and $u_i u_j$ signifies the Reynolds stress tensor.

These equations are solved in a coupled manner to predict velocity, pressure, and other flow parameters at each computational point in the domain. Specifically, the equations are solved using the pressure implicit method with splitting of operators for pressure-linked equations (PIMPLE) algorithm. The PIMPLE algorithm combines two classical methods: the pressure implicit with splitting of operators (PISO) algorithm and the semi-implicit method for pressure-linked equations (SIMPLE) algorithm. This hybrid approach allows for efficient time-stepping in transient simulations, while ensuring both stability and accuracy.

The PIMPLE algorithm works by iterating between pressure and velocity corrections within each time step. The primary steps include a pressure prediction, followed by a correction of both the velocity and pressure fields, allowing for the pressure-velocity coupling to be resolved. The algorithm uses multiple iterations within each time step, improving accuracy, particularly in unsteady and turbulent flow simulations, which are common in tidal turbine applications. In the context of tidal turbines, where flow conditions can vary dynamically, the PIMPLE algorithm ensures that the flow remains incompressible, capturing turbulence and accurately simulating the turbine's interaction with the tidal flow. This iterative process enables stable and efficient simulations, making it well-suited for modeling the complex flow behavior around turbine blades under realistic tidal conditions.

3.2. Turbulence model

In CFD simulations, turbulence models are concepts to accurately capture the behavior of turbulent flows, which are commonly encountered in many engineering applications, including tidal turbine simulations. Turbulence models provide a way to approximate the effects of turbulent eddies and other chaotic flow structures on the fluid flow. Turbulence models are necessary because solving the NS equations directly for turbulent flows would require prohibitively high computational resources. Common turbulence models used in tidal turbine simulations include the k-epsilon (k- ϵ) and k-omega (k- ω) models. Both of these models belong to the Reynolds-averaged Navier-Stokes (RANS) category of turbulence models. They are referred to as two-equation RANS models because they solve two additional transport equations: one for turbulent kinetic energy (k) and the other for either the dissipation rate (ϵ) in the k- ϵ model or the specific dissipation rate (ω) in the k- ω model. These models simplify the turbulence problem by averaging the fluctuating flow quantities, allowing them to effectively represent time-averaged turbulent flow behavior in simulations while still capturing the primary effects of turbulence on the fluid motion. In this study, the k- ϵ turbulence model is employed because it is well-suited for identifying issues related to fluid flow through

complex geometries [21]. The model's ability to handle fully developed turbulent flows efficiently makes it ideal for simulating the interactions between the tidal flow and the turbine blades, which involve intricate geometrical features. Additionally, the k- ϵ model strikes a balance between accuracy and computational efficiency, making it a practical choice for the analysis of turbulent flow characteristics in the case of marine hydrodynamic loads, including the case of tidal turbine performance in this study. Ferziger *et al.* [22] showed k- ϵ turbulent model in (6). The eddy viscosity of turbulence is determined as in (7).

$$\frac{\partial(\rho\epsilon)}{\partial t} + \frac{\partial(\rho u_j \epsilon)}{\partial x_j} = C_{\epsilon 1} P_k \frac{\epsilon}{k} - \rho C_{\epsilon 2} \frac{\epsilon^2}{k} + \frac{\partial}{\partial x_j} \left(\frac{\mu_t}{\sigma_\epsilon} \frac{\partial \epsilon}{\partial x_j} \right) \quad (6)$$

$$\mu_t = \rho C_\mu \sqrt{k} L = \rho C_\mu \frac{k^2}{\epsilon} \quad (7)$$

This model contains five parameters; the most commonly used values for them are:

$$C_\mu = 0.09; C_{\epsilon 1} = 1.44; C_{\epsilon 2} = 1.92; \sigma_k = 1.0; \sigma_\epsilon = 1.3$$

Where k represents the intensity of the turbulence and is associated with the energy contained in turbulent eddies, while ϵ represents the rate at which turbulent kinetic energy is converted into thermal energy due to viscous forces. The k- ϵ model is suitable for moderate to high Reynolds number flows and is often used in industrial applications. It is particularly effective for flows with fully developed turbulence but may not perform well for low-Reynolds-number flows or flows with significant separation or recirculation.

3.3. Meshing

In CFD simulations, meshing is a critical step that involves discretizing the computational domain into small cells, allowing the solver to approximate the fluid flow equations numerically. For simulating HATT using OpenFOAM, meshing is particularly important because of the complex geometry and the need for high accuracy in capturing flow behavior around the turbine blades and within the surrounding fluid domain. The first step in the meshing process is defining the computational domain, which is typically a large volume of water through which the tidal flow will pass. This domain includes the inlet (where the tidal flow enters), the region around the turbine blades, and the outlet where the flow exits. The next step is to import the geometry of the HATT, which includes the turbine blades, hub, into the computational domain. In this study, the model does not include supporting structures. The overall computational domain, including the HATT, is depicted in Figure 2. From Figure 2, it can be seen that the CFD domain is constructed from two regions, which are rotating and stationary zones. The stationary zone is represented by a rectangular form with two distinct cell sizes, as seen in Figure 2(a), whereas Figure 2(b) shows the circular region, which represents the rotary zone. The region that intersects between the stationary and rotary zones is the interface cells. Smaller cell sizes are employed around the blade to enhance simulation accuracy, thus affecting to result's precision. However smaller size produces a high number of generated cells, which strongly influences the computational effort. The desired mesh in this paper was generated using the CFMesh software. The software enables efficient parallelization using shared memory parallelization (SMP) and distributed memory parallelization with message passing interface (MPI) [23]. The rotating mesh is developed with the function of a dynamic mesh library in OpenFOAM. The library provides an interface creation to set a surface boundary between rotating and stationary zones, as shown in Figure 2(c). The HATT model is located inside the rotating zone. The cells inside the zone rotate along with the turbine rotor rotation. In a meshing process, one should ensure that the generated mesh is of good quality. This can be obtained by evaluating the checking mesh feature (checkMesh). The outcome yields a total of 316,894 cells with negligible error. Detailed mesh properties are outlined in a mesh statistic shown in Table 1, along with the mesh quality assessment derived from the checkMesh command in OpenFOAM.

The presented Table 1 elucidates that the generated cells predominantly consist of hexahedra with 1,196,560 cells in total. The structured nature of these cells, as supported by the reference provided by Kumar *et al.* [24], is known to enhance accuracy and stability in simulation outcomes. With this abundance of cells, an effective simulation setup can be established. Moreover, minimizing skewness values ensures improved mesh quality, thereby contributing to more reliable simulation results. Meanwhile, the rotary zone assumes a cylindrical form, with a tighter mesh configuration aimed at eliminating any gaps between the stationary and rotary zones. Cyclic arbitrary mesh interface (cyclicAMI) is applied at the cylindrical interface section to facilitate seamless interaction between the stationary and rotary zones. Communication across topologically different patches is made possible via arbitrary mesh interface (AMI) cyclic patches, which build interpolation weights based on the fractional overlap of faces on each side of the linked patch [19]. The BC has several settings based on references [21], [25], [26].

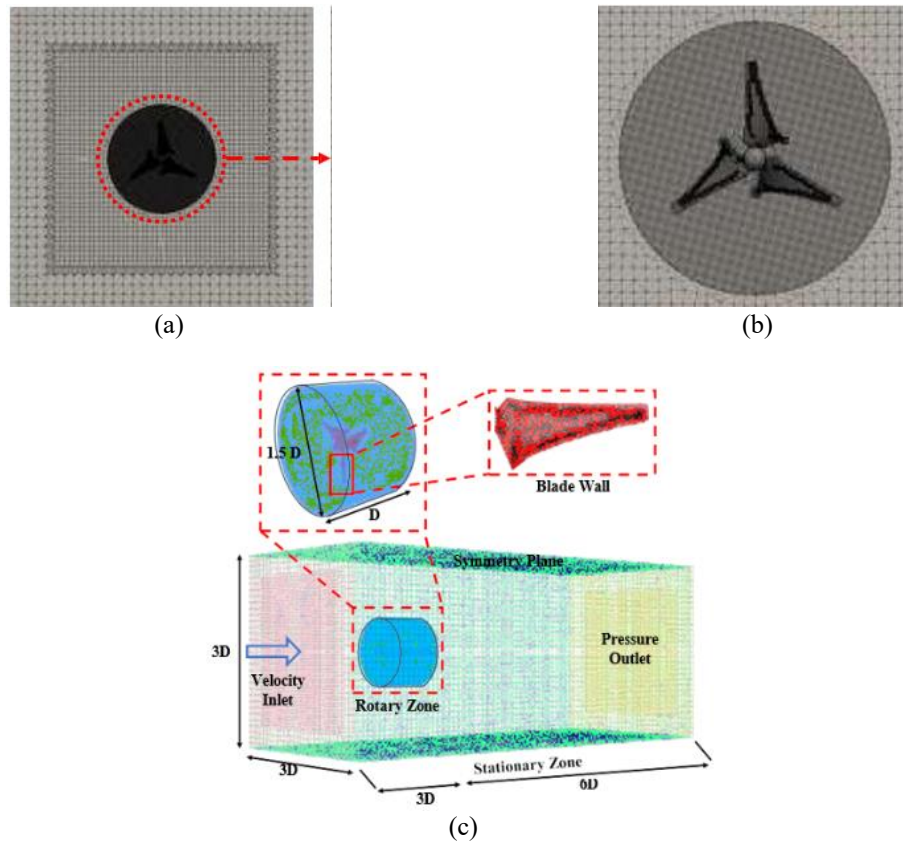


Figure 2. Front view of mesh generation of (a) domain mesh, (b) cylinder with dynamic mesh, and (c) computational domain with BC

Table 1. Mesh quality

Element	Value
Cell	1,196,560
Max cell openness	3.18609e-16
Max aspect ratio	7.29071
Mesh non-orthogonality average	2.99293
Max skewness	2.5264

3.4. Boundary condition

In CFD simulations of HATT using OpenFOAM, BC governs the behavior of the flow at the boundaries of the computational domain. Defining appropriate BC is essential for accurate results, thus ensuring that the interaction between the tidal current and the turbine is modeled correctly. Typical BC used in HATT simulations are inlet BC, outlet BC, wall BC, and BC for the dynamic mesh. The dynamic mesh is employed to handle the interface mesh between the stationary and rotary zones.

The computational domain of the three-dimensional turbine is illustrated in Figure 2(c). As explained, the domain is developed from two subdomains: the stationary zone and the rotary zone. The stationary zone represents the region of the domain that remains fixed, while the rotary zone corresponds to the area where the blade rotation occurs. The dynamic mesh employs cyclicAMI techniques to seamlessly connect the stationary and rotary zones. The stationary domain features a length of $9D$ with D as the turbine diameter. This is characterized by an elongated box shape where the extended downstream region is located. The inlet zone is designated by a velocity inlet, with dimensions of $3D$ in both length and width. Conversely, the outlet is defined as a pressure outlet with specified inlet dimensions. Symmetry plane conditions are imposed on the sides. On the other hand, the rotary domain exhibits a diameter of $1.5D$ and a length of $1D$, positioned within a $3D$ inlet form. The blade BC is characterized by a wall with no-slip conditions.

A dynamic mesh is used in the CFD simulation of HATT to accurately represent the turbine's motion and the surrounding fluid flow. Since HATTs involve rotating blades interacting with tidal currents, a well-designed mesh captures the dynamic movement of the blades and the flow field efficiently, minimizing

computational cost and inaccuracies. In this approach, only the region surrounding the turbine moves, rather than the entire computational domain.

4. RESULTS AND DISCUSSION

Results of the HATT CFD simulation are determined after defining the flow equations, turbulence model, meshing strategy, and BC. The pimpleFOAM solver iteratively solves the fluid flow equations using a time-stepping approach, making adjustments to the velocity, pressure, and turbulence fields at each time step. The simulation is run across a range of TSRs to evaluate the turbine performance under different operating conditions. By varying the TSR, the optimal operating point can be determined for each turbine design (NACA 2415 and OptA) and their performance in terms of power generation, torque, and efficiency. Other techniques to predict the performance in terms of power generation, torque, and efficiency are to analyze the velocity contour, which is detailed in the following section. Velocity contour analysis is a powerful visualization technique for understanding fluid dynamics, as it helps to interpret complex flow fields and hydrodynamic forces. By using contour plots, the thrust and power can be analyzed.

4.1. Velocity contour analysis

Velocity contour plots provide critical insights into the flow characteristics around the turbine blades and the surrounding fluid. These plots are an essential tool for understanding how the tidal current interacts with the rotating turbine and how the turbine extracts energy from the fluid flow. Velocity contours allow for the visualization of the speed and direction of the fluid at different points in the HATT blades, highlighting regions of high and low flow velocities. By analyzing the contours near the blades, it is possible to observe how the flow accelerates, decelerates, or changes direction due to the presence of the blades. The velocity contour also helps to identify areas of the flow where the velocity is significantly reduced, indicating regions where the turbine blades are extracting energy from the fluid.

In regions where the flow detaches from the blade surface, the velocity drops significantly, leading to flow separation. Velocity contours can help identify these areas and visualize the extent of separation, which can cause drag and reduce the efficiency of the turbine. By examining the velocity contours for flow separation, blade geometry, and twist distribution can be optimized to reduce these effects, improving the lift-to-drag ratio and overall efficiency. The velocity contours can highlight these vortices in the wake region, which is caused by separation. By analyzing the velocity contours, phenomena can be identified, which is essential for understanding how the turbine impacts the surrounding flow field and harnesses energy. This also assesses how quickly the flow recovers after passing through the turbine and how the vortices and wake affect other turbines in a potential tidal farm arrangement. If the velocity distribution across the blades is uneven, it may indicate areas where blade design or twist distribution can be improved to enhance performance. One can identify areas where flow stagnation occurs or where the fluid is efficiently channeled through the rotor, contributing to power generation. The velocity contour of various TSR on each foil as a result of simulations in this study is shown in Figure 3.

Figures 3(a) and 3(b) show the flow behavior in three different TSRs (TSR=4, 5, and 6) in the surroundings of turbines using NACA 2415 and OptA blades, respectively. The tidal velocity for both models is 2 m/s, which is assumed to be BC at the fluid inlet. Performance comparison of turbine (Figure 4), the vortices in Figures 4(a) and 4(b) can be analyzed by observing the flow characteristics behind the turbines. At TSR 4, both foils exhibit flow separation, which can be seen from the fluid detachment at the downflow region, but there is no significant disruptive flow visible in the figure. This suggests that NACA 2415 maintains stable flow conditions at lower TSR values. This indicates that the turbine using NACA 2415 has similar flow phenomena in low tidal speed to OptA, thus it is likely that both performances are much more the same. As the TSR increases from 4 to 6, changes in vortex formation become more pronounced. At lower TSR values, both designs exhibit stable flow, but as TSR increases, the difference in flow separation becomes more noticeable, leading to increased turbulence and energy dissipation, particularly in the NACA 2415 design. Flow separation in the downstream flow region is more distinct and stronger in NACA 2415 compared to OptA. In contrast, OptA shows a thickened fluid stream, indicating more efficient energy capture.

At TSR 5, a noticeable difference emerges between the OptA and NACA 2415 turbines. The NACA 2415 turbine begins to experience disruptive flow, likely caused by flow separation at the blade's trailing edge. In contrast, the OptA turbine exhibits smoother flow behavior, with minimal separation along the blade. This finding aligns with the ducted turbine concept, which aims to streamline the flow behind the turbine blades. Research conducted by Rahmatian *et al.* [27] on ducted turbines demonstrated that adding a duct structure significantly improves C_p by minimizing turbulence and optimizing wake flow characteristics. As TSR increases, the disruptive flow becomes more prominent. At TSR 6, the vortex formation is evident along the blade surface in both foils. While OptA maintains better vortex control and experiences less disruption than NACA 2415, some degree of turbulence still occurs, reducing overall turbine efficiency at

high TSR values. Efficient vortex control is crucial for maintaining smooth energy extraction and minimizing power losses. The reduced vortex shedding in the OptA turbine suggests that modifications to foil design and flow conditioning strategies can significantly enhance overall turbine performance. Overall, the OptA turbine exhibits a more stable distribution and improved vortex control compared to NACA 2415, leading to higher efficiency and reduced energy losses. These findings emphasize the role of foil modifications in optimizing tidal turbine performance under varying operational conditions.

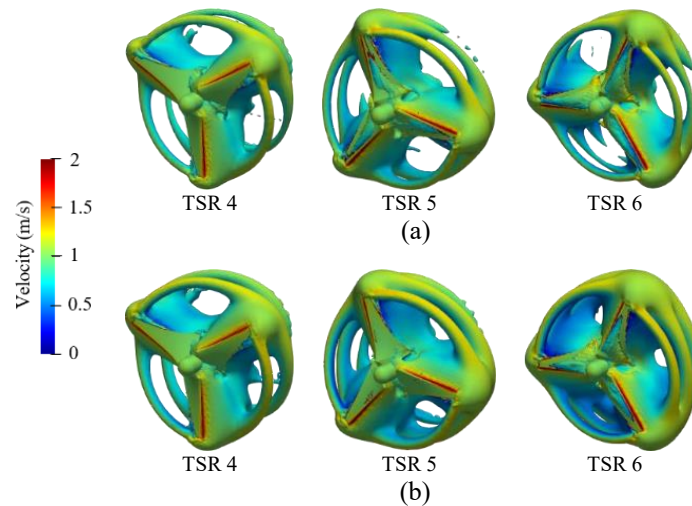


Figure 3. Velocity contour between (a) NACA 2415 and (b) OptA turbine

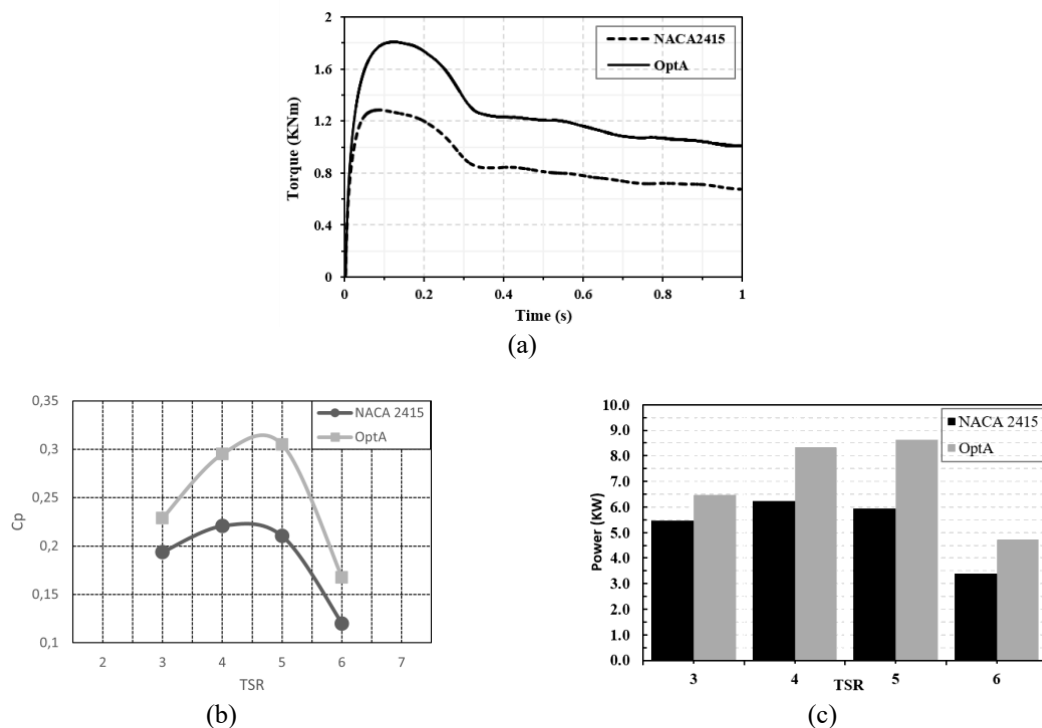


Figure 4. Performance comparison of the turbine of (a) torque at TSR 5, (b) C_p turbine in different TSR, and (c) power is produced at different TSRs

It was observed that greater twist distribution in the OptA blade design is associated with a reduction in vortex formation. The approach used in this study consistently showed significantly better ability to maintain

flow velocity in the downstream area as the twist angle increased, especially at TSR values of 5 and 6. These findings indicate that the combination of effective flow conditioning and optimized blade geometry in the OptA design provides a substantial benefit in enhancing tidal energy conversion efficiency.

At higher TSR, the performance differences between the NACA 2415 and OptA foils become more apparent. As the TSR increases, the flow dynamics around the turbine blades change, particularly at the trailing edge of the blade. In the case of the OptA foil, the velocity at the trailing edge drops more significantly compared to the NACA 2415 foil. This reduction in velocity indicates a more efficient energy extraction process because the turbine blades rotate with a higher speed at slowing down the flow, converting more kinetic energy from the tidal current into mechanical energy for rotation. However, at the leading edge of both foils, the velocity profiles remain largely similar, suggesting that the initial flow interaction with the blades is not significantly affected by the foil design at higher TSRs. The key difference lies in how the foils handle the flow as it moves along the blade towards the trailing edge. In OptA, the thicker flow near the trailing edge indicates improved energy capture, suggesting that the foil's design and twist distribution optimize the interaction between the fluid and the blade surface. This results in a better conversion of tidal energy into rotational energy.

The enhanced performance of the OptA foil can be attributed to its ability to maintain a more favorable lift-to-drag ratio and minimize flow separation, particularly at higher TSRs. This allows the turbine to operate more efficiently, generating more torque and power. The efficiency in converting tidal energy to mechanical power leads to a more stable and consistent turbine operation, which is crucial for the long-term viability of tidal energy systems.

4.2. Performance analysis

In this study, turbine performance is analyzed based on torque and C_p , as these parameters directly impact the energy extraction efficiency of the turbine. Torque is a fundamental performance metric that determines the mechanical power output of the turbine. Comparison of performance across various parameters is illustrated in Figure 4. Figure 4(a) presents a detailed comparison of the torque history for both the NACA 2415 and OptA turbines.

It can be observed that the torque peak occurs at 0.1 seconds, marking the onset of the simulation. This peak represents an initial period of instability caused by the turbine's inertia and its interaction with the fluid flow before transitioning into a steady state. This transient behavior highlights the dynamic nature of turbine operation, where higher initial torque is generated due to the interplay of mechanical forces within the system. The initial peak torque of the NACA 2415 turbine is 1.28 kNm, while the OptA turbine exhibits a higher peak of 1.81 kNm, representing a 41.4% increase in torque output for the OptA turbine.

The increase in torque for the OptA turbine can be attributed to its modified foil shape, which enhances lift while minimizing drag-induced losses. This improvement results in greater momentum transfer from the fluid to the turbine blades, increasing the mechanical power output. As the simulation progresses, the torque gradually stabilizes. By 0.3 seconds, the turbine begins to transition towards a steady state, with the torque decreasing slightly as stability is attained. At 1 second, the torque output fully stabilizes. The stabilization of torque after 1 second indicates that the turbine reaches a consistent rotational state, directly influencing the C_p values across different TSRs. The stable torque ensures a more efficient energy conversion process, reflected in the higher C_p values achieved by the OptA turbine. Additionally, the torque values indicate that the NACA 2415 foil also possesses self-starting capabilities, which aligns with the findings of Beri and Yao in their study on vertical axis turbines (VATs) [28].

Meanwhile, Figure 4(b) illustrates the C_p values of both the OptA and NACA 2415 turbines across different TSR, ranging from 3 to 6. The graph in Figure 4(b) depicts the C_p characteristics over one full turbine rotation. At a design flow rate of 2 m/s, the OptA turbine consistently exhibits higher C_p values across all TSR ranges. As the TSR increases, the C_p value also increases until reaching TSR 5. This increase is attributed to the turbine's rising angular velocity, which enhances energy extraction through rotation. TSR 5 is identified as the optimal design point, as indicated by the highest C_p values recorded. The OptA turbine reaches a C_p value of 0.303, outperforming the NACA 2415 turbine, which achieves a C_p value of 0.210. This reflects a 40.2% increase in C_p for the OptA turbine. The significance of TSR 5 as the peak performance point can be attributed to the balance between rotational speed and inflow velocity, which maximizes energy extraction while avoiding excessive drag forces that reduce efficiency at higher TSRs. However, as TSR reaches 6, both turbines experience a significant decline in performance, indicating that they have surpassed their optimal operating conditions. The C_p evaluation is directly related to power production, as shown in Figure 4(c).

Turbine power production varies across different TSR values, as shown in Figure 4(c). The OptA turbine demonstrates superior power generation across all TSR ranges, reinforcing its improved performance over NACA 2415. However, other studies on NACA 2415 foils applied to Darrieus-type VATs have achieved peak C_p values of 0.409 at TSR 1.75 with a wind speed of 7 m/s and a C_p of 0.36 at 4 m/s [29]. While previous studies have shown NACA 2415 achieving high C_p values in Darrieus-type VATs, these results may not directly translate to HATT applications due to differences in flow mechanics. The performance of

NACA 2415 in HATTs must therefore be assessed independently to determine its suitability in tidal energy applications. Furthermore, additional studies suggest that turbine solidity plays a crucial role in determining C_p , particularly in vertical-axis configurations [30]. This emphasizes the importance of considering design-specific optimizations when applying foil modifications to different types of tidal turbines.

Overall, the OptA turbine demonstrates superior performance in both torque generation and energy extraction efficiency. It achieves a 40.2% increase in C_p compared to the NACA 2415 turbine. These results highlight the importance of optimized foil designs in enhancing tidal turbine performance, emphasizing the need for further investigations into foil modifications for specific operational environments.

5. CONCLUSION

This study aimed to evaluate the performance of HATT using NACA 2415 and OptA foils, focusing on torque, C_p , and flow characteristics. Through numerical simulations conducted in OpenFOAM, the impact of foil modifications and twist distributions on turbine efficiency was analyzed across different TSRs. The results confirm that the OptA turbine significantly outperforms the NACA 2415 turbine, demonstrating a 41.4% increase in torque and a 40.2% increase in C_p at the optimal operating condition of TSR 5. The velocity contour analyses revealed that the OptA foil produces a more uniform velocity distribution and reduced flow separation, leading to enhanced energy extraction. Additionally, the vortex structure behind the OptA turbine exhibited smoother flow behavior, minimizing disruptive turbulence that can negatively affect turbine stability. Although this study provides a detailed comparison of blade geometry and twist distribution impacts on turbine performance, additional research is required to verify the consistency of these findings under diverse flow environments and through experimental validation. This becomes increasingly critical when considering full-scale implementation and prolonged exposure to turbulent marine conditions. Additionally, future studies should consider the interaction between structural deformation and hydrodynamic forces by applying a coupled CFD-finite element method (FEM) approach. It will also be important to assess the material selection, fatigue resistance, and manufacturability of the optimized blades to ensure real-world viability. Overall, the enhanced performance observed in the OptA turbine appears to result from better flow regulation and minimized separation due to refined geometric design. These findings strengthen the idea that targeted modifications to foil shape have a more significant impact on efficiency improvements than merely enlarging blade dimensions.

FUNDING INFORMATION

The authors confirm that no external funding was received for the execution of this study. All research activities, including data collection, simulations, and analysis, were conducted independently without financial support from any institution, organization, or funding agency.

AUTHOR CONTRIBUTIONS STATEMENT

This journal uses the Contributor Roles Taxonomy (CRediT) to recognize individual author contributions, reduce authorship disputes, and facilitate collaboration.

Name of Author	C	M	So	Va	Fo	I	R	D	O	E	Vi	Su	P	Fu
Nu Rhahida Arini	✓	✓	✓	✓	✓	✓				✓		✓		
Philips Ade Putera	✓		✓		✓				✓		✓			
Atmojo														
Deni Saputra					✓	✓	✓	✓		✓			✓	
Dendy Satrio		✓		✓			✓		✓			✓		

C : **C**onceptualization

M : **M**ethodology

So : **S**oftware

Va : **V**alidation

Fo : **F**ormal analysis

I : **I**ntellectual

R : **R**esources

D : **D**ata Curation

O : **O**riginal Draft

E : **E**diting

Vi : **V**isualization

Su : **S**upervision

P : **P**roject administration

Fu : **F**unding acquisition

CONFLICT OF INTEREST STATEMENT

The authors declare that there are no known conflicts of interest, financial or otherwise, that could have influenced the outcomes of this research. No personal or professional relationships exist that may have impacted the objectivity or validity of the study.

DATA AVAILABILITY

The authors affirm that all data supporting the findings of this study are included within the article and its supplementary materials. Additional datasets or computational models used in the research can be made available upon reasonable request.




REFERENCES

- [1] IEA, "Energy statistics data browser," *International Energy Agency*. Accessed: Mar. 31, 2024. [Online]. Available: <https://www.iea.org/data-and-statistics/data-tools/energy-statistics-data-browser>
- [2] M. Azam, A. Q. Khan, K. Zaman, and M. Ahmad, "Factors determining energy consumption: evidence from Indonesia, Malaysia and Thailand," *Renewable and Sustainable Energy Reviews*, vol. 42, pp. 1123–1131, Feb. 2015, doi: 10.1016/j.rser.2014.10.061.
- [3] M. H. Hasan, T. M. I. Mahlia, and H. Nur, "A review on energy scenario and sustainable energy in Indonesia," *Renewable and Sustainable Energy Reviews*, vol. 16, no. 4, pp. 2316–2328, May 2012, doi: 10.1016/j.rser.2011.12.007.
- [4] Republic of Indonesia, *Government regulation (PP) no. 79 of 2014 concerning national energy policy (in Indonesian: Peraturan pemerintah (PP) nomor 79 tahun 2014 tentang kebijakan energi nasional)*. 2014. [Online]. Available: <https://peraturan.bpk.go.id/Details/5523/pp-no-79-tahun-2014>
- [5] L. Myers and A. S. Bahaj, "Power output performance characteristics of a horizontal axis marine current turbine," *Renewable Energy*, vol. 31, no. 2, pp. 197–208, Feb. 2006, doi: 10.1016/j.renene.2005.08.022.
- [6] Y. Dong *et al.*, "An adaptive yaw method of horizontal-axis tidal stream turbines for bidirectional energy capture," *Energy*, vol. 282, Nov. 2023, doi: 10.1016/j.energy.2023.128918.
- [7] A. Boudis, O. Guerri, A.-C. B.-Lainé, H. Oualli, A. Benzaoui, and O. C.-Delgosha, "Investigations on the use of a KFM-4 profile to improve the energy extraction performance of a fully-activated flapping foil," *Ocean Engineering*, vol. 295, p. 116980, Mar. 2024, doi: 10.1016/j.oceaneng.2024.116980.
- [8] J. N. Goundar and M. R. Ahmed, "Design of a horizontal axis tidal current turbine," *Applied Energy*, vol. 111, pp. 161–174, Nov. 2013, doi: 10.1016/j.apenergy.2013.04.064.
- [9] G. Tefera, G. Bright, and S. Adali, "Theoretical and computational studies on the optimal positions of NACA airfoils used in horizontal axis wind turbine blades," *Journal of Energy Systems*, vol. 6, no. 3, pp. 369–386, Sep. 2022, doi: 10.30521/jes.1055935.
- [10] R. Alipour, R. Alipour, F. Fardian, and M. H. Tahan, "Optimum performance of a horizontal axis tidal current turbine: a numerical parametric study and experimental validation," *Energy Conversion and Management*, vol. 258, Apr. 2022, doi: 10.1016/j.enconman.2022.115533.
- [11] A. Gray, B. Singh, and S. Singh, "Low wind speed airfoil design for horizontal axis wind turbine," *Materials Today: Proceedings*, vol. 45, pp. 3000–3004, 2021, doi: 10.1016/j.matpr.2020.11.999.
- [12] Z. Sun, Y. Mao, and M. Fan, "Performance optimization and investigation of flow phenomena on tidal turbine blade airfoil considering cavitation and roughness," *Applied Ocean Research*, vol. 106, Jan. 2021, doi: 10.1016/j.apor.2020.102463.
- [13] N. R. Arini, G. Muhammad, J. Pratilastiarso, E. Tridianto, B. Sumantri, and S. Nugroho, "Prediction on the maximum lift force of twisted Clark Y wind turbine blade with 30° winglet tip in various pitch angles using CFD method," *IOP Conference Series: Earth and Environmental Science*, vol. 1121, no. 1, Dec. 2022, doi: 10.1088/1755-1315/1121/1/012010.
- [14] Z. Sun, D. Li, Y. Mao, L. Feng, Y. Zhang, and C. Liu, "Anti-cavitation optimal design and experimental research on tidal turbines based on improved inverse bem," *Energy*, vol. 239, Jan. 2022, doi: 10.1016/j.energy.2021.122263.
- [15] B. E. Abuan and R. J. Howell, "The performance and hydrodynamics in unsteady flow of a horizontal axis tidal turbine," *Renewable Energy*, vol. 133, pp. 1338–1351, Apr. 2019, doi: 10.1016/j.renene.2018.09.045.
- [16] M. A. Rotor and H. Hefazi, "Design and simulation of a horizontal-axis tidal turbine (HATT) blades for tropical site conditions using Reynolds-averaged Navier-Stokes - blade element momentum theory (RANS-BEMT)," in *OCEANS 2021: San Diego – Porto*, IEEE, Sep. 2021, pp. 1–9. doi: 10.23919/OCEANS44145.2021.9705826.
- [17] M. H. Khanjanpour and A. A. Javadi, "Optimization of a horizontal axis tidal (HAT) turbine for powering a reverse osmosis (RO) desalination system using computational fluid dynamics (CFD) and Taguchi method," *Energy Conversion and Management*, vol. 231, Mar. 2021, doi: 10.1016/j.enconman.2021.113833.
- [18] C. Ariza, C. Casado, R.-Q. Wang, E. Adams, and J. Marugán, "Comparative evaluation of openfoam® and ansys® fluent for the modeling of annular reactors," *Chemical Engineering & Technology*, vol. 41, no. 7, pp. 1473–1483, Jul. 2018, doi: 10.1002/ceat.201700455.
- [19] S. Vilfayeau, C. Pesci, S. Ferraris, A. Heather, and F. Roesler, "Improvement of arbitrary mesh interface (AMI) algorithm for external aerodynamic simulation with rotating wheels," in *Fourth international conference in Aerovehicles 4-2021 numerical and experimental aerodynamics of road vehicles and trains*, Berlin, Germany, 2021, pp. 1-4.
- [20] S. Rahgozar, A. Pourrajabian, S. A. A. Kazmi, and S. M. R. Kazmi, "Performance analysis of a small horizontal axis wind turbine under the use of linear/nonlinear distributions for the chord and twist angle," *Energy for Sustainable Development*, vol. 58, pp. 42–49, Oct. 2020, doi: 10.1016/j.esd.2020.07.003.
- [21] D. Satrio *et al.*, "The influence of deflector on the performance of cross-flow Savonius turbine," *International Review on Modelling and Simulations*, vol. 16, no. 1, p. 27, Feb. 2023, doi: 10.15866/iremos.v16i1.22763.
- [22] J. H. Ferziger, M. Perić, and R. L. Street, *Computational methods for fluid dynamics*. Cham, Switzerland: Springer International Publishing, 2020. doi: 10.1007/978-3-319-99693-6.
- [23] F. Juretić, *CfMesh v1.1: user guide*. Creative Fields, 2015. [Online]. Available: https://cfmesh.com/wp-content/uploads/2015/09/User_Guide-cfMesh_v1.1.pdf
- [24] M. Kumar, G. W. Nam, S. J. Oh, J. Seo, A. Samad, and S. H. Rhee, "Design optimization of a horizontal axis tidal stream turbine blade using CFD," in *Fifth International Symposium on Marine Propulsors*, Espoo, Finland, 2017, pp. 1-8.
- [25] D. Satrio, S. Suntoyo, E. Erwandhi, F. Albatinusa, T. Tuswan, and M. L. Hakim, "The benefit using a circular flow disturbance on the Darrieus turbine performance," *International Journal on Engineering Applications*, vol. 11, no. 1, Jan. 2023, doi: 10.15866/irea.v11i1.22434.
- [26] S. Junianto, W. N. Fadilah, A. F. Adila, Tuswan, D. Satrio, and S. Musabikha, "State of the art in floating tidal current power plant using multi-vertical-axis-turbines," in *2022 International Electronics Symposium*, IEEE, Aug. 2022, pp. 97–103, doi: 10.1109/IES55876.2022.9888749.




- [27] M. A. Rahmatian, P. H. Tari, M. Mojaddam, and S. Majidi, "Numerical and experimental study of the ducted diffuser effect on improving the aerodynamic performance of a micro horizontal axis wind turbine," *Energy*, vol. 245, Apr. 2022, doi: 10.1016/j.energy.2022.123267.
- [28] H. Beri and Y. Yao, "Numerical simulation of unsteady flow to show self-starting of vertical axis wind turbine using Fluent," *Journal of Applied Sciences*, vol. 11, no. 6, pp. 962–970, Mar. 2011, doi: 10.3923/jas.2011.962.970.
- [29] S. Chhin and V. S. Djanali, "Numerical simulation on hybrid Savonius turbine with NACA-airfoils as H-rotor blades," in *2020 International Seminar on Intelligent Technology and Its Applications*, IEEE, Jul. 2020, pp. 123–128. doi: 10.1109/ISITIA49792.2020.9163710.
- [30] J. D. C.-Cárdenas, D. A. H. Zuluaga, J. G. A. Marín, R. de O. Faria, and C. A. R. Vanegas, "Impact of blade and solidity on the performance of H-Darrieus hydrokinetic turbines by CFD simulation," *Revista de Gestão Social e Ambiental*, vol. 18, no. 1, Oct. 2023, doi: 10.24857/rgsa.v18n1-007.

BIOGRAPHIES OF AUTHORS






Nu Rhahida Arini    is an Associate Professor in Power Plant Engineering at the Department of Mechanical Engineering and Energy, Politeknik Elektronika Negeri Surabaya (PENS), Indonesia. She earned her Ph.D. from the Civil, Maritime, and Environmental Engineering and Science Unit at the University of Southampton, UK, and holds a master's degree in Mechanical Engineering from the Bandung Institute of Technology (ITB), Indonesia. Her research focuses on the development of sustainable energy solutions for remote islands in Indonesia, with particular expertise in the design and performance evaluation of wind and tidal energy systems. Her areas of interest include fluid dynamics and computational fluid dynamics (CFD), particularly using OpenFOAM. She has led numerous collaborative research projects with both academic and industrial partners. Her contributions to renewable energy research have earned her national and international recognition, including being named a finalist for the Underwriters Laboratories ASEAN-U.S. Science Prize for Women 2023. She can be contacted at email: arini@pens.ac.id.






Philips Ade Putera Atmojo    graduated with an undergraduate degree in Power Plant Engineering from Politeknik Elektronika Negeri Surabaya in 2022. He is currently working in the instrumentation industry in Gresik City. His research interests include renewable energy turbines, computational fluid dynamics (CFD), and the application of NACA profiles in turbines and aviation. He can be contacted at email: philiputerade@gmail.com.



Deni Saputra    is currently an undergraduate student specializing in Power Plant Engineering at Politeknik Elektronika Negeri Surabaya. His research interests include renewable energy, particularly in turbines, turbulence modeling, and computational fluid dynamics. He can be contacted at email: denisaputra0411@gmail.com.



Dendy Satrio    is an Associate Professor at the Department of Ocean Engineering, Faculty of Marine Technology, Institut Teknologi Sepuluh Nopember (ITS), Surabaya, Indonesia. He received his Ph.D. in Ocean Energy Engineering from ITS and his D-4 degree in Energy Generation Systems from Politeknik Elektronika Negeri Surabaya (PENS-ITS). His research interests include energy conversion, marine renewable energy, computational fluid dynamics (CFD), and experimental fluid dynamics. He can be contacted at email: dendy.satrio@its.ac.id.